ORIGINAL RESEARCH

Annals of Internal Medicine

Autopsy Findings and Venous Thromboembolism in Patients With COVID-19

A Prospective Cohort Study

Dominic Wichmann, MD*; Jan-Peter Sperhake, MD*; Marc Lütgehetmann, MD; Stefan Steurer, MD; Carolin Edler, MD; Axel Heinemann, MD; Fabian Heinrich; Herbert Mushumba, MD; Inga Kniep, MD; Ann Sophie Schröder, MD; Christoph Burdelski, MD; Geraldine de Heer, MD; Axel Nierhaus, MD; Daniel Frings, MD; Susanne Pfefferle, MD; Heinrich Becker, MD; Hanns Bredereke-Wiedling, MD; Andreas de Weerth, MD; Hans-Richard Paschen, MD; Sara Sheikhzadeh-Eggers, MD; Axel Stang, MD; Stefan Schmiedel, MD; Carsten Bokemeyer, MD; Marylyn M. Addo, MD, PhD; Martin Aepfelbacher, MD; Klaus Püschel, MD†; and Stefan Kluge, MD†

Background: The new coronavirus, severe acute respiratory syndrome coronavirus 2 (SARS-CoV-2), has caused more than 210 000 deaths worldwide. However, little is known about the causes of death and the virus's pathologic features.

Objective: To validate and compare clinical findings with data from medical autopsy, virtual autopsy, and virologic tests.

Design: Prospective cohort study.

Setting: Autopsies performed at a single academic medical center, as mandated by the German federal state of Hamburg for patients dying with a polymerase chain reaction–confirmed diagnosis of COVID-19.

Patients: The first 12 consecutive COVID-19–positive deaths.

Measurements: Complete autopsy, including postmortem computed tomography and histopathologic and virologic analysis, was performed. Clinical data and medical course were evaluated.

Results: Median patient age was 73 years (range, 52 to 87 years), 75% of patients were male, and death occurred in the hospital (n = 10) or outpatient sector (n = 2). Coronary heart disease and asthma or chronic obstructive pulmonary disease were the most common comorbid conditions (50% and 25%, respectively). Autopsy revealed deep venous thrombosis in 7 of 12 patients (58%) in whom venous thromboembolism was not suspected before death; pulmonary embolism was the direct cause of death in 4 patients. Postmortem computed tomography revealed reticular infiltration of the lungs with severe bilateral, dense consolidation, whereas histomorphologically diffuse alveolar damage was seen in 8 patients. In all patients, SARS-CoV-2 RNA was detected in the lung at high concentrations; viremia in 6 of 10 and 5 of 12 patients demonstrated high viral RNA titers in the liver, kidney, or heart.

Limitation: Limited sample size.

Conclusion: The high incidence of thromboembolic events suggests an important role of COVID-19–induced coagulopathy. Further studies are needed to investigate the molecular mechanism and overall clinical incidence of COVID-19–related death, as well as possible therapeutic interventions to reduce it.

Primary Funding Source: University Medical Center Hamburg-Eppendorf.

Ann Intern Med. 2020;173:268-277. doi:10.7326/M20-2003 **Annals.org**
For author, article, and disclosure information, see end of text.
This article was published at Annals.org on 6 May 2020.
* Drs. Wichmann and Sperhake share first authorship.
† Drs. Püschel and Kluge share last authorship.

Since it was first detected in December 2019, the novel severe acute respiratory syndrome coronavirus 2 (SARS-CoV-2) spread from the central Chinese province of Hubei to almost every country in the world (1, 2). Most persons with COVID-19 have a mild disease course, but about 20% develop a more severe course with a high mortality rate (3). As of 26 April 2020, more than 2.9 million persons have been diagnosed with COVID-19 and 210 000 of them have died (4). Why the new coronavirus seems to have a much higher mortality rate than the seasonal flu is not completely understood. Some authors have reported potential risk factors for a more severe disease course, including elevated D-dimer levels, a high Sequential Organ Failure Assessment score, and older age (5, 6). Because of the novelty of the pathogen, little is known about the causes of death in affected patients and its specific pathologic features. Despite modern diagnostic tests, autopsy is still of great importance and may be a key to understanding the biological characteristics of SARS-CoV-2 and the pathogenesis of the disease. Ideally, knowledge gained in this way can influence therapeutic strategies and ultimately reduce mortality. To our knowledge, only 3 case reports have been published about COVID-19 patients who have undergone complete autopsy (7, 8). Therefore, in this study we investigated the value of autopsy for determining the cause of death and describe the pathologic characteristics in patients who died of COVID-19.

METHODS

Study Design

In response to the pandemic spread of SARS-CoV-2, the authorities of the German federal state of Hamburg ordered mandatory autopsies in all patients dying with a diagnosis of COVID-19 confirmed by polymerase chain reaction (PCR). The legal basis for this was section 25(4) of the German Infection Protection Act. Because of legal regulations, no COVID-19 death was exempted from this order, even if its clinical cause seemed obvious. The case series demonstrated herein consists of 12 consecutive autopsies, starting with the first known

SARS-CoV-2–positive death occurring in Hamburg (the second largest city in Germany, with 1.8 million inhabitants). All autopsies were performed at the Department of Legal Medicine of University Medical Center Hamburg-Eppendorf. The Ethics Committee of the Hamburg Chamber of Physicians was informed about the study (no. WF-051/20). The study was approved by the local clinical institutional review board and complied with the Declaration of Helsinki. In all deceased patients, postmortem computed tomography (PMCT) and a complete autopsy, including histopathologic and virologic evaluation, were performed. Clinical records were checked for preexisting medical conditions and medications, current medical course, and antemortem diagnostic findings.

PMCT, Autopsy, and Histologic Examination

Computed tomographic examination was done at the Department of Legal Medicine with a Philips Brilliance 16-slice multidetector scanner in accordance with an established protocol (9). In brief, full-body computed tomography was performed from top to thigh (slice thickness, 1 mm; pitch, 1.5; 120 kV; 230 to 250 mAs), complemented by dedicated scans of the thorax with higher resolution (slice thickness, 0.8 mm; pitch, 1.0; 120 kV; 230 to 250 mAs). We performed external examinations and full-body autopsies on all deceased persons with SARS-CoV-2 positivity (PCR confirmed) as soon as possible after taking proper safety precautions (using personal protective equipment with proper donning and doffing), following guidelines from the German Association of Pathologists, which are closely aligned with relevant international guidelines. The recently published recommendations for the performance of autopsies in cases of suspected COVID-19 were taken into account (10). The interval from death to postmortem imaging and autopsy (postmortem interval) ranged from 1 to 5 days. During autopsy, tissue samples for histology were taken from the following organs: heart, lungs, liver, kidneys, spleen, pancreas, brain, prostate and testes (in males), ovaries (in females), small bowel, saphenous vein, common carotid artery, pharynx, and muscle.

For virologic testing, we took small samples of heart, lungs, liver, kidney, saphenous vein, and pharynx and sampled the venous blood.

Tissue samples for histopathologic examination were fixed in buffered 4% formaldehyde and processed via standard procedure to slides stained with hematoxylin–eosin. For the lung samples, we also used the keratin marker AE1/AE3 (Dako) for immunohistochemistry.

Quantitative SARS-CoV-2 RNA Reverse Transcription PCR From Tissue

Tissue samples were ground by using ceramic beads (Precellys lysing kit) and extracted by using automated nucleic acid extraction (MagNA Pure 96 [Roche]) according to manufacturer recommendations. For virus quantification in tissues, a previously published assay was adopted with modifications (11). One-step real-time PCR was run on the LightCycler 480 system (Roche) by using a 1-step RNA control kit (Roche) as master mix. The C_t (cycle threshold) value for the target SARS-CoV-2 RNA (fluorescein) and whole-process RNA control (Cy5) was determined by using the second derivative maximum method. For quantification, standard in vitro–transcribed RNA of the E gene of SARS-CoV-2 was used (12). These samples were also analyzed in a study focusing on renal tropism of SARS-CoV-2 (Puelles V, et al. Multi-organ and renal tropism of SARS-CoV-2. In preparation).

Statistical Analysis

Data that were normally distributed are presented as means (SDs); data outside the normal distribution are presented as medians (ranges). Categorical variables were summarized as counts and percentages. All data were analyzed with Statistica, version 13 (StatSoft).

Role of the Funding Source

The sponsor was not involved in the design or conduct of the study, nor in the analysis of the data or the decision to submit the manuscript.

RESULTS

Clinical Data

The median age of the 12 patients included in this study was 73 years (interquartile range, 18.5 years); 25% were women. For all patients, preexisting chronic medical conditions, such as obesity, coronary heart disease, asthma or chronic obstructive pulmonary disease, peripheral artery disease, diabetes mellitus type 2, and neurodegenerative diseases, could be identified (Table 1). Two patients died out of the hospital after unsuccessful cardiopulmonary resuscitation, 5 died after treatment in the intensive care unit, and the remaining 5 had an advanced directive for best supportive care and died in the non–intensive care ward. Laboratory results for clinical chemistry, hematology, and coagulation were not available for the patients who died out of the hospital. In the remaining patients, the most striking features of the initial laboratory test were elevated levels of lactate dehydrogenase (median, 7.83 μkat/L [range, 2.71 to 11.42 μkat/L]), D-dimer (available for 5 patients; median, 495.24 nmol/L [range, 20.38 to >1904.76 nmol/L]), and C-reactive protein (median, 189 mg/L [range, 18 to 348 mg/L]), as well as mild thrombocytopenia in 4 of 10 patients. A procalcitonin test had been performed in 6 patients, and the results were negative in all but 1 patient with pneumonia (case 10). Table 2 provides an overview of the initial laboratory results.

Postmortem Computed Tomography

In 2 cases (2 and 4), PMCT was not possible for logistic reasons. In the remaining cases, PMCT demonstrated mixed patterns of reticular infiltrations and severe, dense, consolidating infiltrates in both lungs in the absence of known preexisting pathology (such as emphysema or tumor). A juxtaposition of antemortem and postmortem findings is demonstrated in Figure 1.

Table 1. Patient Characteristics and Autopsy Findings

Case Number	Age, *y*	Sex	Preexisting Medical Conditions	Treatment	BMI, *kg/m²*	Clinical Cause of Death	PMI, *d*
1	52	Male	Obesity	CPR	38.8	Sudden cardiac death	1
2	70	Male	Parkinson disease, CHD, PAD, CKD	BSC	22.2	Respiratory failure, pneumonia	1
3	71	Male	AH, nicotine abuse, granulomatous pneumopathy	CA, MV	36.8	Respiratory failure, pneumonia	2
4	63	Male	T2DM, obesity, bronchial asthma	CA, MV, lysis of right ventricular thrombus, CPR	37.3	Cardiorespiratory failure, PE	1
5	66	Male	CHD	CPR	25.3	Sudden cardiac death	2
6	54	Female	Dementia, epilepsy, trisomy 21	BSC	29.6	Respiratory failure, aspiration pneumonia	1
7	75	Female	Atrial fibrillation, CHD, nicotine abuse	NIV	26.3	Respiratory failure, viral pneumonia	4
8	82	Male	Parkinson disease, T2DM, CHD	BSC	27.8	Respiratory failure, viral pneumonia	1
9	87	Female	Non–small cell lung cancer, COPD, CHD, CKD	BSC	15.4	Respiratory failure, viral pneumonia	4
10	84	Male	T2DM, AH, ulcerative colitis	BSC	20.7	Respiratory failure, viral pneumonia	5
11	85	Male	CHD, AH, bronchial asthma, atrial fibrillation	CA, MV, RRT	30.0	Cardiac arrest due to respiratory failure	2
12	76	Male	Obesity	CA, MV, CPR	34.4	PE	3

AB = acute bronchitis; ACVB = aortocoronary venous bypass; AH = arterial hypertension; aPC = activated pneumocytes; BMI = body mass index; BSC = best supportive care; CA = catecholamine therapy; CB = chronic bronchitis; CHD = coronary heart disease; CKD = chronic kidney disease; Co = congestion of small vessels; COPD = chronic obstructive pulmonary disease; CPR = cardiopulmonary resuscitation; DAD = diffuse alveolar damage; DVT = deep venous thrombosis; FB = fibroblasts; GC = giant cells; Gra = granulocytic infiltration; HI = hemorrhagic infarctions; HM = hyaline membranes; LAD = left anterior descending artery; LC = lymphocytes; MI = myocardial infarction; MV = mechanical ventilation; NET = neuroendocrine tumor; NIV = noninvasive ventilation; PAD = peripheral artery disease; PE = pulmonary embolism; PEG = percutaneous endoscopic gastrostomy; PlC = plasma cells; PMCT = postmortem computed tomography; PMI = postmortem interval; RCA = right coronary artery; RRT = renal replacement therapy; SM = squamous metaplasia; T2DM = type 2 diabetes mellitus; Thr = thrombi; VATS = video-assisted thoracoscopic surgery.

A complete summary of PMCT findings is presented in Table 1.

Autopsy

In 4 cases (1, 3, 4, and 12), massive pulmonary embolism was the cause of death, with the thrombi deriving from the deep veins of the lower extremities. In another 3 cases (5, 8, and 11), fresh deep venous thrombosis was present in the absence of pulmonary embolism. In all cases with deep venous thrombosis, both legs were involved (Figure 2). In 6 of the 9 men

Table 1–Continued

Cause of Death	Main Pathologic Findings	PMCT (Lungs)	Histology (Lungs)
PE, pneumonia	PE, DVT, pneumonia, obesity, cardiomegaly (660 g), splenomegaly (500 g), hepatomegaly (3880 g), shock organs (liver, kidneys), atherosclerosis	Diffuse bilateral pulmonary consolidations in each lobe	DAD: aPC, FB, GC, sparse HM, slight fibrosis Additional findings: Co, Thr
Pneumonia with bronchopneumonia	Pneumonia, CHD (stents in LAD and RCA, status post MI, cardiac aneurysm), contractures (with Parkinson syndrome), purulent bronchitis, cardiomegaly (515 g), shock liver	No PMCT	DAD: aPC, HM, sparse LC Additional findings: focal Gra, CB, AB
PE, pneumonia	PE, DVT, pneumonia, status post VATS (due to unspecified granuloma), CHD, anasarca, atherosclerosis	Emphysema; fine reticular pattern in each lobe; consolidations in the right lower and left lower lobes	DAD: SM, FB, aPC, HM Additional findings: Thr
PE, pneumonia	PE, DVT, pneumonia, obesity, cardiomegaly (605 g), ischemic colitis, shock liver	No PMCT	DAD: FB, aPC, HM, SM Additional findings: HI, Thr
Pneumonia	Pneumonia, DVT, CHD, status post MI	Consolidations in each lobe; reticular pattern in the right upper and lower lobes and in each left lobe	DAD: aPC, FB, HM, necrosis, LC Additional findings: surrounding small vessels, Thr
Pneumonia	Pneumonia, kidney infarctions, PEG tube	Consolidations in the right upper and middle lobes and in parts of the left upper and lower lobes; ground glass opacities in the right upper and lower lobes and in the left upper lobe; reticular pattern in the right middle and lower lobes and in each left lobe	Gra, AB, Co (no DAD)
Pneumonia	Pneumonia, lung emphysema, CHD, left cardiac dilatation, calcification of the mitral ring, cardiac pacemaker, atherosclerosis	Reticular pattern in each lobe; small areas of consolidation in the right lower, left upper, and left lower lobes	DAD: HM, aPC, SM Additional findings: emphysema, Co
Bronchopneumonia	Pneumonia, emphysema, DVT, CHD, status post ACVB, status post MI with left cardiac aneurysm, atherosclerosis	Emphysema; diffuse consolidations in each lobe; reticular pattern in the right upper and lower lobes and in the left lower lobe; bilateral pleural effusion	Gra, emphysema (no DAD)
Purulent bronchitis	Pneumonia, purulent bronchitis, CHD, status post MI, cachexia, bullous emphysema, NET in the lung, atherosclerosis	Emphysema; round tumor in the right lower lobe; small areas of consolidation in the right upper and lower lobes and in the left upper lobe; reticular pattern in the right upper and lower lobes and in each left lobe	Gra, AB, emphysema (no DAD) Additional findings: NET composed of small cells
Pneumonia, septic encephalopathy	Pneumonia, emphysema, septicemia, status post MI, atrophic kidneys	Reticular pattern in the right upper and lower lobes and in each left lobe; consolidations in the right middle and lower lobes and in each left lobe; ground glass opacities in the right upper and middle lobes and in parts of the left upper lobe; bilateral pleural effusion	Emphysema, Co, Gra, CB, fibrosis (no DAD)
Pneumonia	Pneumonia, DVT, minor PE, emphysema, CHD, cardiomegaly (650 g), atherosclerosis	Diffuse consolidations in each lobe; reticular pattern in the right middle and lower lobes and in each left lobe; ground glass opacities in the right upper and middle lobes and in the left upper lobe; bilateral pleural effusion	DAD: HM (sparse), GC, aPC Additional findings: emphysema, Co, Gra
PE	PE with lung infarctions, DVT, pneumonia, purulent tracheobronchitis, pneumonia, cardiomegaly (745 g), emphysema, obesity	No residual ventilation in either lung except for small areas in the right upper and middle lobes and in the left upper and lower lobes; bilateral pleural effusion	DAD: HM, aPC, fibrosis Additional findings: LC, PIC, HI, Thr, Co

(two thirds) included in the study, fresh thrombosis was also present in the prostatic venous plexus (**Appendix Figure 1**, available at Annals.org).

In all 12 cases, the cause of death was found within the lungs or the pulmonary vascular system. However, macroscopically differentiating viral pneumonia with subsequent diffuse alveolar damage (a histologic diagnosis) from bacterial pneumonia was not always possible. Typically, the lungs were congested and heavy, with a maximum combined lung weight of 3420 g in case 11. The mean combined lung weight was 1988 g (median, 2088 g). Standard lung weights for men and women are 840 g and 639 g, respectively (13, 14). Only cases 6 and 9 presented with a relatively low lung weight: 550 g and 890 g, respectively (**Appendix Table 1**, available at Annals.org). The lung surface often displayed mild pleurisy and a distinct patchy pattern, with pale areas alternating with slightly protruding and firm, deep reddish blue hypercapillarized areas. On the cutting surfaces, this pattern was also visible (**Figure 2**).

Table 2. Overview of Laboratory Results Taken at the Time of Hospitalization*

Case Number	Hemoglobin, *g/dL*	MCV, *fL*	Platelets, $\times 10^9$/*L*	Leukocytes, $\times 10^9$/*L*	INR	aPTT, *s*	D-dimer, *μg/L*	LDH, *μkat/L*	Creatinine, *μmol/L*
Normal range	14.0–17.5	80.0–94.0	150–400	3.8–11.0	–	23–30	<500	2.00–4.10	53.4–99.1
1	NA	NA	NA	NA	NA	NA	NA	NA	NA
2	12.1	92	144	7.4	1.3	NA	NA	5.92	228.8
3	14.9	100	190	9.2	2.1	42	NA	6.32	102.9
4	13.3	88	478	7.1	1.1	21	23 100	11.07	65.6
5	14.4	NA	NA	NA	NA	NA	NA	NA	NA
6	14.0	95	135	3.4	1.0	30	NA	6.12	59.5
7	12.1	98	125	6.9	1.5	57	28 800	7.97	76.3
8	14.8	79	186	7.1	1.2	29	2100	9.84	99.1
9	10.7	98	210	5.3	1.0	23	NA	2.70	99.1
10	16.5	88	219	15.5	1.1	29	>200 000	10.50	129.6
11	9.9	78	304	11.6	1.1	45	5700	11.40	83.9
12	16.8	90	141	3.8	0.95	32	NA	6.32	67.1

aPTT = activated partial thromboplastin time; AST = aspartate aminotransferase; CRP = C-reactive protein; INR = international normalized ratio; LDH = lactate dehydrogenase; MCV = mean corpuscular volume; NA = not available; PCT = procalcitonin.
* Patients in cases 1 and 5 died out of the hospital after a sudden cardiac arrest. Values are either nonexistent (case 1) or taken from a blood gas analysis (case 5).

The consistency of the lung tissue was firm yet friable. In 8 cases, all parts of the lungs were affected by these changes. Cases 6, 7, and 9—occurring in the 3 women of the case series—presented with changes compatible with focal purulent bronchopneumonia. Macroscopically, no changes were observed outside the lungs and respiratory tract, except for splenomegaly in 3 cases, which suggested a viral infection.

During autopsy, all cases except for case 6 presented with preexisting heart disease, including high-grade coronary artery sclerosis (7 of 12); myocardial scarring, indicating ischemic heart disease (6 of 12); and congestive cardiomyopathy. Mean heart weight was 503 g (median, 513 g). In addition to this finding, the most common accompanying diseases were pulmonary emphysema (6 of 12) and ischemic enteritis (3 of 12). Often these conditions were known to the treating physician before death (compare columns 4 and 10 of Table 1). The macroscopic autopsy findings are presented organ by organ in Appendix Table 2 (available at Annals.org) and the lung findings in Table 1.

A clear trend toward obesity was observed among the cases (mean body mass index, 28.7 kg/m^2; median, 28.7 kg/m^2). However, case 9, involving a patient with known neuroendocrine tumor of the lung, presented with severe cachexia (body mass index, 15.4 kg/m^2). The comorbid conditions found are summarized in Table 1.

Histology

Histopathology of the lungs showed diffuse alveolar damage, consistent with early acute respiratory distress syndrome in 8 cases. Predominant findings were hyaline membranes (Figure 3, *A* and *B*), activated pneumocytes, microvascular thromboemboli, capillary congestion, and protein-enriched interstitial edema. As described by Wang and colleagues (15), a moderate degree of inflammatory infiltrates concurred with clinically described leukopenia in patients with COVID-19 and predominant infiltration of lymphocytes fit the picture of a viral pathogenesis. In later stages, squamous metaplasia was present (Figure 3, *C*). Long-term changes, such as destruction of alveolar septae and lymphocytic infiltration of the bronchi, were often visible as preexisting conditions. Four cases (6, 8, 9, and 10) showed no diffuse alveolar damage but extensive granulocytic infiltration of the alveoli and bronchi, resembling bacterial focal bronchopneumonia. Histologically, thromboemboli were detectable in cases 1, 3, 4, and 5 (Figure 3, *D*). Microthrombi were regularly found within small lung arteries, occasionally within the prostate, but not in other organs.

In addition to the lung changes described in Table 1, there were isolated histologic findings that might indicate a viral infection. The pharyngeal mucosa was examined in 7 cases. In 6 of them, hyperemia and alternating dense, predominantly lymphocytic infiltrates were found as signs of chronic pharyngitis. In 1 case (case 3), lymphocytic myocarditis was seen in the right ventricle (Appendix Figure 2, available at Annals.org). The remaining histologic changes were compatible with shock changes in part of the deceased patient (liver, kidneys, intestine) or corresponded to the macroscopically determined virus-independent preexisting pathology (such as ischemic cardiomyopathy).

Apart from findings related to SARS-CoV-2 infection, patients showed other histopathologic findings related to their chronic preexisting conditions, including hypertrophy of myocardial fibers or scarring of the myocardium. The peripheral veins, including those occluded by thrombi, showed no abnormalities on hematoxylin–eosin staining.

PCR Results

Quantitative reverse transcription PCR detected SARS-CoV-2 RNA in the lungs of all 12 patients (range, 1.2×10^4 to 9×10^9 copies/mL) and in the pharynx of 9 patients. Six patients showed moderate viremia ($<4 \times 10^4$ copies/mL). In 5 of these patients, viral RNA was also detected in other tissues (heart, liver, or kid-

Table 2–Continued

AST, *U/L*	Sodium, *mmol/L*	Potassium, *mmol/L*	CRP, *mg/L*	PCT, *mg/L*	Antimicrobial and Coagulation Therapy
<50	135–145	3.6–4.6	<5	<0.5	
NA	NA	NA	NA	NA	None
54	154	4.6	303	NA	Rivaroxaban: 20 mg once daily Piperacillin/tazobactam: 4.5 g three times daily
52	139	4.45	304	NA	Meropenem: 1 g three times daily Levofloxacin: 400 mg twice daily Enoxaparin: 4000 IU once daily
54	139	3.5	133	0.1	Cefpodoxime: 200 mg twice daily
NA	141	8.7	NA	NA	None
NA	132	4.4	18	0.2	None
97	141	3.8	213	0.3	Edoxaban: 30 mg once daily
NA	141	4.6	92	NA	None
NA	135	4.6	39	NA	None
NA	140	3.5	348	16.2	None
77	141	4.5	268	0.3	None
77	136	4.3	167	0.5	Certoparin: 3000 IU once daily

ney) in concentrations exceeding viremia. Patients without viremia showed no or a low virus load in the other tissues. Only 4 patients had detectable viral RNA in the brain and saphenous vein.

Discussion

In this autopsy study of 12 consecutive patients who died of COVID-19, we found a high incidence of deep venous thrombosis (58%). One third of the patients had a pulmonary embolism as the direct cause of death. Furthermore, diffuse alveolar damage was demonstrated by histology in 8 patients (67%).

To our knowledge, this is the first case series summarizing and comparing clinical data of consecutive COVID-19 cases with findings obtained by a full autopsy, supplemented by PMCT, histology, and virology.

The high rate of death-causing pulmonary embolism at autopsy correlates well with the unsuccessful resuscitation of 3 of 4 patients, 2 of whom died out of the hospital. Apart from that, no preclinical evidence had been reported of pulmonary embolism or deep venous thrombosis.

In studies that examined deceased patients with COVID-19 without relying on autopsy, no increased rates of pulmonary embolism were observed clinically. However, it is known that many cases of pulmonary embolism remain clinically overlooked and are often associated with sudden, unexpected death. This may have been aggravated by the method for diagnosing COVID-19 in Germany, which is based on PCR tests rather than computed tomographic imaging because of concerns about infection of medical staff and other patients. A recent report described clinical features of 85 fatal cases of COVID-19 from Wuhan (16). Besides respiratory failure, the cause of death was multiorgan failure in 16% and cardiac arrest in 9%. No autopsies were performed. The gold standard for identifying cause of death is still the autopsy (17). However, in-hospital autopsy rates have declined worldwide over the past decades. Also, because of pathologists' potential risk for SARS-CoV-2 infection, very few autopsies

Figure 1. Antemortem versus postmortem computed tomographic (CT) imaging (case 3).

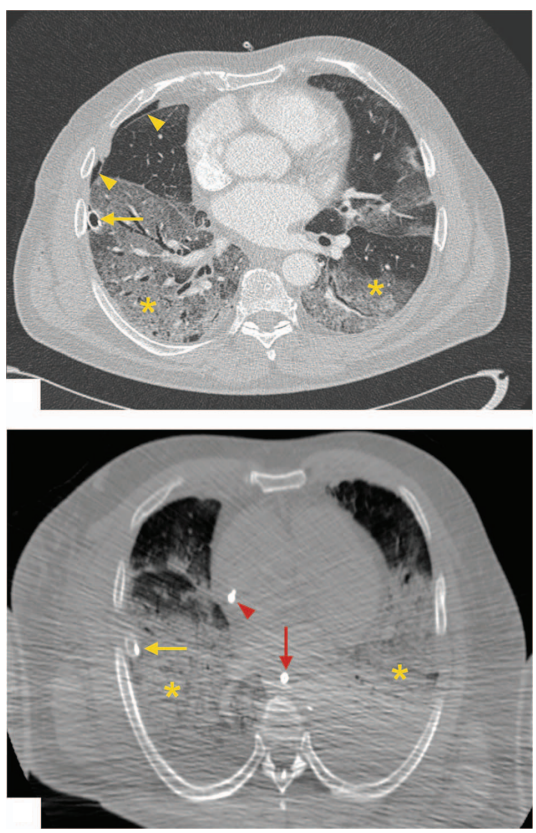

Top. Contrast medium–enhanced CT scan demonstrates the antemortem findings: bilateral ground glass opacities in the lower lobes of both lungs (*yellow asterisks*) and a chest tube (*yellow arrow*), which has been introduced to treat a pneumothorax (*yellow arrowheads*). **Bottom.** CT scan without contrast medium enhancement demonstrates the corresponding postmortem findings. For technical reasons, the postmortem image has a lower resolution. To protect the staff from potential infection, bodies were scanned in a double-layer body bag with the arms positioned alongside the body. Although the findings correspond to the antemortem images, ground glass opacities in both lower lobes (*yellow asterisks*) and a chest tube (*yellow arrow*) are seen. In addition, a central venous line (*red arrowhead*) and gastric tube (*red arrow*) are visible.

have been performed worldwide (18). To our knowledge, only 3 case reports have been published on patients with COVID-19 who have undergone complete autopsy and a few more in which only lung tissue was examined (7, 8).

Other researchers have described coagulopathy as a common complication in patients with severe COVID-19 (5, 6, 19). In a recent study of 191 patients with COVID-19, 50% of those who died had coagulopathy, compared with 7% of survivors. D-dimer levels greater than 1000 μg/L were associated with a fatal outcome (6).

COVID-19 may predispose to venous thromboembolism in several ways. The coagulation system may be activated by many different viruses, including HIV, dengue virus, and Ebola virus (20, 21). In particular, coronavirus infections may be a trigger for venous thromboembolism, and several pathogenetic mechanisms are involved, including endothelial dysfunction, characterized by increased levels of von Willebrand factor; systemic inflammation, by Toll-like receptor activation; and a procoagulatory state, by tissue factor pathway activation (22). In a subgroup of patients with severe COVID-19, high plasma levels of proinflammatory cytokines were observed (23). The direct activation of the coagulation cascade by a cytokine storm is conceivable. With COVID-19, severe hypoxemia develops in some patients (24). Thrombus formation under hypoxic conditions is facilitated both in animal models of thrombosis and in humans. The vascular response to hypoxia is controlled primarily by the hypoxia-inducible transcription factors, whose target genes include several factors that regulate thrombus formation (25). Lastly, indirect causes, such as immune-mediated damage by antiphospholipid antibodies, may partially contribute, as speculated by Zhang and colleagues (26).

The macroscopic findings in our autopsy series—with rather heavy, consolidated, friable, basically air-free lungs in most of the cases—were impressive and explain the difficulties in sufficiently ventilating some of these patients. The histopathologic changes in most of our cases with diffuse alveolar damage as the main finding resemble those described by Xu and colleagues (7) and Barton and colleagues (8), who reported single cases; Zhang and colleagues (26), who reported on lung biopsy in a patient with SARS-CoV-2 positivity; and Tian and colleagues (27), who described macroscopic and histologic pulmonary findings in 2 patients with lung cancer who received positive results on SARS-CoV-2 testing. However, the full-blown picture of diffuse alveolar damage seems to be more prevalent in younger patients with fewer preexisting diseases and longer survival, whereas older patients with more comorbid conditions tend to die in the early stages of the disease.

In line with clinical, macroscopic, and histopathologic findings, PCR detected the highest concentration of SARS-CoV-2 RNA in lung and pharyngeal tissue. Of interest, in most patients with disease, high titers of RNA were also detected in postmortem samples. The clinical relevance of this is not yet clear. Clearance of viral RNA from blood 7 days after transfusion of

Figure 2. Macroscopic autopsy findings.

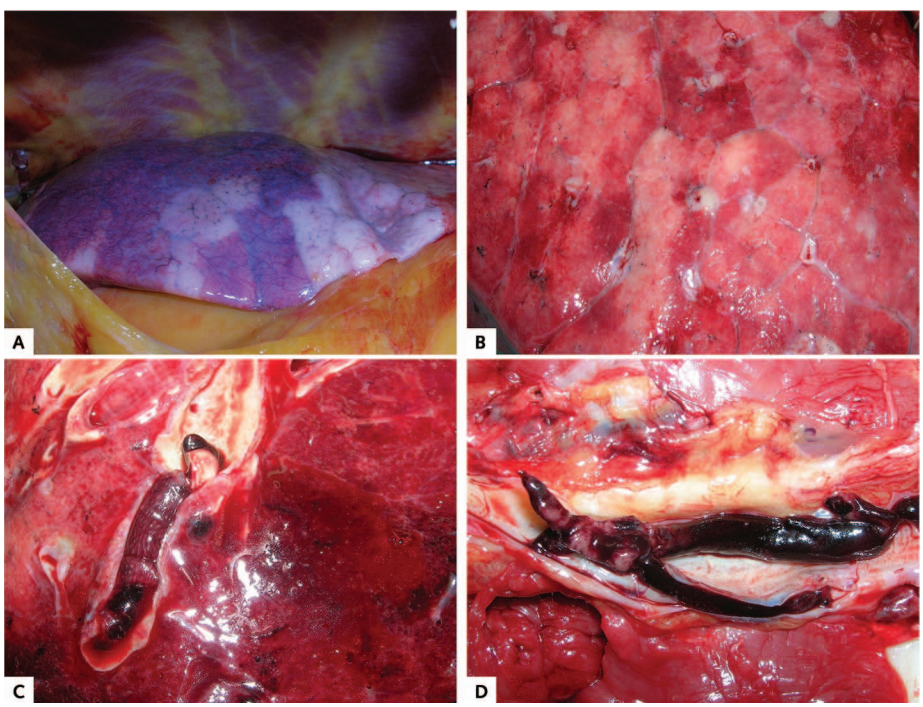

A. Patchy aspect of the lung surface (case 1). **B.** Cutting surface of the lung in case 4. **C.** Pulmonary embolism (case 3). **D.** Deep venous thrombosis (case 5).

Figure 3. Histopathologic findings.

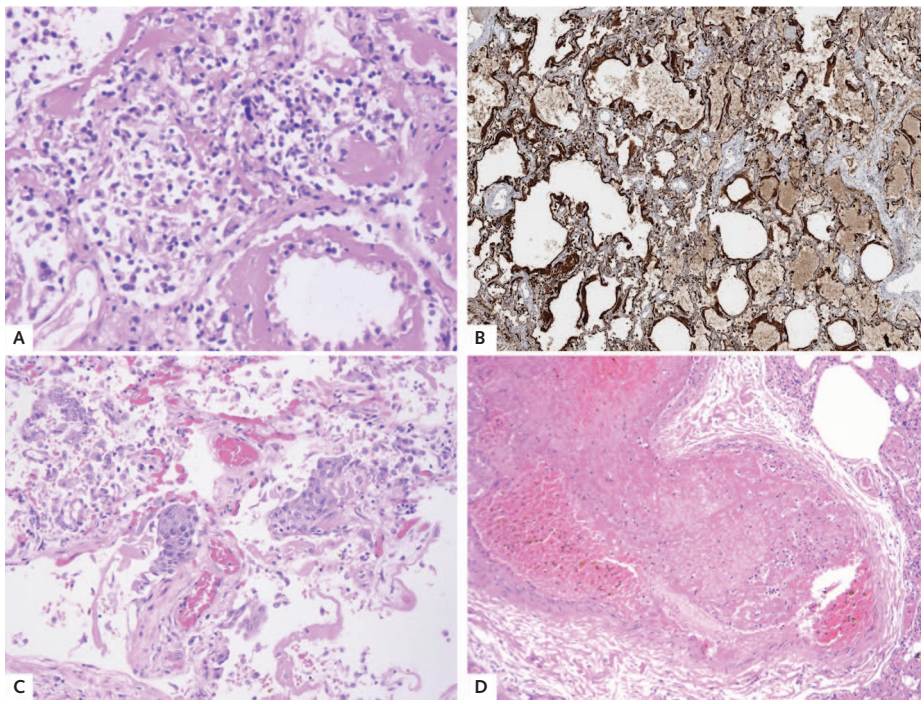

A. Diffuse alveolar damage with hyaline membranes (case 4) (hematoxylin–eosin [H&E] stain; original magnification, × 50). **B.** Hyaline membranes (case 4) (cytokeratin AE1/AE3 stain; original magnification, × 50). **C.** Squamous metaplasia in the lung (case 5) (H&E stain; original magnification, × 100). **D.** Pulmonary embolism (case 1) (H&E stain; original magnification, × 100).

COVID-19 convalescent plasma was associated with substantial clinical improvement, but studies have not shown a correlation between viremia and acute respiratory distress syndrome in patients with severe COVID-19 (28, 29). As in patients with SARS-CoV-1, in whom viral replication could be detected in other organs, including the liver, kidney, spleen, and cerebrum (30), we detected viral RNA at high titers in other organs (liver, kidney, and heart) in 5 patients. These data suggest that SARS-CoV-2 may spread via the bloodstream and infect other organs. To prove this, replication intermediates must be detected.

The current study had some limitations. First, the sample size was small, possibly leading to overestimation of the rate of pulmonary embolism. However, both the clinical and postmortem observations agree well with the current knowledge about SARS-CoV-2 pathology. This includes the sex and age distribution as well as the preexisting conditions among the patients, but also the histologic findings. Second, although viral titers in swabs (pharynx) taken longitudinally up to 7 days after death remained similar, we lack data on how postmortem processes affect viral titers and dynamics in different tissues and body fluids. Moreover, the quantitative PCR assay used cannot discriminate between genomic and subgenomic RNA. As stated earlier, to prove viral replication, detection of replication intermediates or antigenomic RNA would be necessary.

In conclusion, we found a high incidence of thromboembolic events in patients with COVID-19. When hemodynamic deterioration occurs in a patient with COVID-19, pulmonary embolism should always be suspected. That patients with COVID-19 who have increased D-dimer levels, a sign of coagulopathy, may benefit from anticoagulant treatment seems plausible (31). As demonstrated in our cohort, this might be important for hospitalized patients and outpatients. In this context, some professional societies have already made recommendations for antithrombotic therapy for patients with COVID-19 (32). Robust evidence, however, remains scant, and further prospective studies are urgently needed to confirm and validate these results.

From University Medical Center Hamburg-Eppendorf, Hamburg, Germany (D.W., J.S., M.L., S.S., C.E., A.H., F.H., H.M., I.K., A.S.S., C.B., G.D., A.N., D.F., S.P., S.S., C.B., M.M.A., M.A., K.P., S.K.); Asklepios Hospital Barmbek, Hamburg, Germany (H.B., A.S.); Bethesda Hospital Bergedorf, Hamburg, Germany (H.B.); Agaplesion Diakonie Hospital, Hamburg, Germany (A.D.); Amalie Sieveking Hospital, Hamburg, Germany (H.P.); and Asklepios Hospital Saint Georg, Hamburg, Germany (S.S.).

Financial Support: By Institutional Funds of University Medical Center Hamburg-Eppendorf, Hamburg, Germany.

Disclosures: Dr. Nierhaus reports grants and personal fees from CytoSorbents Europe and personal fees from Thermo Fisher Scientific and Biotest outside the submitted work. Dr. Frings reports personal fees from Xenios outside the submit-

ted work. Dr. Bokemeyer reports personal fees from Sanofi-Aventis, Merck KgaA, Bristol-Myers Squibb, Merck Sharp & Dohme, Lilly ImClone, Bayer, GSO Contract Research, AOK Rheinland/Hamburg, and Novartis outside the submitted work. Dr. Kluge reports grants from Ambu, E.T. View, Fisher & Paykel, Pfizer, and Xenios and personal fees from Amomed, ArjoHuntleigh, Astellas, Astra, Basilea, Bard, Bayer, Baxter, Biotest, CSL Behring, CytoSorbents, Fresenius, Gilead, MSD, Orion, Pfizer, Philips, Sedana, Sorin, Xenios, and Zoll outside the submitted work. Authors not named here have disclosed no conflicts of interest. Disclosures can also be viewed at www.acponline.org/authors/icmje/ConflictOfInterestForms.do?msNum=M20-2003.

Reproducible Research Statement: *Study protocol:* Available with approval through written agreement with Dr. Wichmann (e-mail, d.wichmann@uke.de). *Statistical code:* Available from Dr. Kluge (e-mail, s.kluge@uke.de). *Data set:* Not available.

Corresponding Author: Dominic Wichmann, MD, Department of Intensive Care Medicine, University Medical Center Hamburg-Eppendorf, Martinistr. 52, 20246 Hamburg, Germany; e-mail, d.wichmann@uke.de.

Current author addresses and author contributions are available at Annals.org.

References

1. **World Health Organization.** Novel coronavirus–China. Accessed at www.who.int/csr/don/12-january-2020-novel-coronavirus-china/en on 26 April 2020.
2. **Zhu N, Zhang D, Wang W, et al; China Novel Coronavirus Investigating and Research Team.** A novel coronavirus from patients with pneumonia in China, 2019. N Engl J Med. 2020;382:727-733. [PMID: 31978945] doi:10.1056/NEJMoa2001017
3. **Wu Z, McGoogan JM.** Characteristics of and important lessons from the coronavirus disease 2019 (COVID-19) outbreak in China: summary of a report of 72 314 cases from the Chinese Center for Disease Control and Prevention. JAMA. 2020. [PMID: 32091533] doi:10.1001/jama.2020.2648
4. **Johns Hopkins University.** Coronavirus Resource Center. COVID-19 Dashboard by the Center for Systems Science and Engineering (CSSE) at Johns Hopkins University (JHU). Accessed at https://coronavirus.jhu.edu/map.html on 26 April 2020.
5. **Tang N, Li D, Wang X, et al.** Abnormal coagulation parameters are associated with poor prognosis in patients with novel coronavirus pneumonia. J Thromb Haemost. 2020;18:844-847. [PMID: 32073213] doi:10.1111/jth.14768
6. **Zhou F, Yu T, Du R, et al.** Clinical course and risk factors for mortality of adult inpatients with COVID-19 in Wuhan, China: a retrospective cohort study. Lancet. 2020;395:1054-1062. [PMID: 32171076] doi:10.1016/S0140-6736(20)30566-3
7. **Xu Z, Shi L, Wang Y, et al.** Pathological findings of COVID-19 associated with acute respiratory distress syndrome. Lancet Respir Med. 2020;8:420-422. [PMID: 32085846] doi:10.1016/S2213-2600(20)30076-X
8. **Barton LM, Duval EJ, Stroberg E, et al.** COVID-19 autopsies, Oklahoma, USA. Am J Clin Pathol. 2020. [PMID: 32275742] doi:10.1093/ajcp/aqaa062
9. **Wichmann D, Obbelode F, Vogel H, et al.** Virtual autopsy as an alternative to traditional medical autopsy in the intensive care unit: a prospective cohort study. Ann Intern Med. 2012;156:123-30. [PMID: 22250143] doi:10.7326/0003-4819-156-2-201201170-00008
10. **Centers for Disease Control and Prevention.** Collection and Submission of Postmortem Specimens from Deceased Persons with Known or Suspected COVID-19, March 2020 (Interim Guidance). Accessed at www.cdc.gov/coronavirus/2019-ncov/hcp/guidance-postmortem-specimens.html on 26 April 2020.
11. **Corman VM, Landt O, Kaiser M, et al.** Detection of 2019 novel coronavirus (2019-nCoV) by real-time RT-PCR. Euro Surveill. 2020;25. [PMID: 31992387] doi:10.2807/1560-7917.ES.2020.25.3.2000045
12. **Romette JL, Prat CM, Gould EA, et al.** The European Virus Archive goes global: a growing resource for research. Antiviral Res. 2018;158:127-134. [PMID: 30059721] doi:10.1016/j.antiviral.2018.07.017
13. **Molina DK, DiMaio VJ.** Normal organ weights in men: part II–the brain, lungs, liver, spleen, and kidneys. Am J Forensic Med Pathol. 2012;33:368-72. [PMID: 22182984] doi:10.1097/PAF.0b013e31823d29ad
14. **Molina DK, DiMaio VJ.** Normal organ weights in women: part II–the brain, lungs, liver, spleen, and kidneys. Am J Forensic Med Pathol. 2015;36:182-7. [PMID: 26108038] doi:10.1097/PAF.0000000000000175
15. **Wang Y, Lu X, Chen H, et al.** Clinical course and outcomes of 344 intensive care patients with COVID-19. Am J Respir Crit Care Med. 2020. [PMID: 32267160] doi:10.1164/rccm.202003-0736LE
16. **Du Y, Tu L, Zhu P, et al.** Clinical features of 85 fatal cases of COVID-19 from Wuhan: a retrospective observational study. Am J Respir Crit Care Med. 2020. [PMID: 32242738] doi:10.1164/rccm.202003-0543OC
17. **Wichmann D, Heinemann A, Weinberg C, et al.** Virtual autopsy with multiphase postmortem computed tomographic angiography versus traditional medical autopsy to investigate unexpected deaths of hospitalized patients: a cohort study. Ann Intern Med. 2014;160:534-41. [PMID: 24733194] doi:10.7326/M13-2211
18. **Hanley B, Lucas SB, Youd E, et al.** Autopsy in suspected COVID-19 cases. J Clin Pathol. 2020;73:239-242. [PMID: 32198191] doi:10.1136/jclinpath-2020-206522
19. **Chen T, Wu D, Chen H, et al.** Clinical characteristics of 113 deceased patients with coronavirus disease 2019: retrospective study. BMJ. 2020;368:m1091. [PMID: 32217556] doi:10.1136/bmj.m1091
20. **Antoniak S, Mackman N.** Multiple roles of the coagulation protease cascade during virus infection. Blood. 2014;123:2605-13. [PMID: 24632711] doi:10.1182/blood-2013-09-526277
21. **Oudkerk M, Büller HR, Kuijpers D, et al.** Diagnosis, prevention, and treatment of thromboembolic complications in COVID-19: report of the National Institute for Public Health of the Netherlands. Radiology. 2020:201629. [PMID: 32324101] doi:10.1148/radiol.2020201629
22. **Giannis D, Ziogas IA, Gianni P.** Coagulation disorders in coronavirus infected patients: COVID-19, SARS-CoV-1, MERS-CoV and lessons from the past. J Clin Virol. 2020;127:104362. [PMID: 32305883] doi:10.1016/j.jcv.2020.104362
23. **Li H, Liu L, Zhang D, et al.** SARS-CoV-2 and viral sepsis: observations and hypotheses. Lancet. 2020. [PMID: 32311318] doi:10.1016/S0140-6736(20)30920-X
24. **Kluge S, Janssens U, Welte T, et al.** German recommendations for critically ill patients with COVID-19. Med Klin Intensivmed Notfmed. 2020. [PMID: 32291505] doi:10.1007/s00063-020-00689-w
25. **Gupta N, Zhao YY, Evans CE.** The stimulation of thrombosis by hypoxia. Thromb Res. 2019;181:77-83. [PMID: 31376606] doi:10.1016/j.thromres.2019.07.013
26. **Zhang H, Zhou P, Wei Y, et al.** Histopathologic changes and SARS-CoV-2 immunostaining in the lung of a patient with COVID-19. Ann Intern Med. 2020. [PMID: 32163542] doi:10.7326/M20-0533
27. **Tian S, Hu W, Niu L, et al.** Pulmonary pathology of early-phase 2019 novel coronavirus (COVID-19) pneumonia in two patients with lung cancer. J Thorac Oncol. 2020;15:700-704. [PMID: 32114094] doi:10.1016/j.jtho.2020.02.010
28. **Duan K, Liu B, Li C, et al.** Effectiveness of convalescent plasma therapy in severe COVID-19 patients. Proc Natl Acad Sci U S A. 2020;117:9490-9496. [PMID: 32253318] doi:10.1073/pnas.2004168117

29. **Dreher M, Kersten A, Bickenbach J, et al.** The characteristics of 50 hospitalized COVID-19 patients with and without ARDS. Dtsch Arztebl Int. 2020;117:271-8.
30. **Ding Y, He L, Zhang Q, et al.** Organ distribution of severe acute respiratory syndrome (SARS) associated coronavirus (SARS-CoV) in SARS patients: implications for pathogenesis and virus transmission pathways. J Pathol. 2004;203:622-30. [PMID: 15141376]
31. **Tang N, Bai H, Chen X, et al.** Anticoagulant treatment is associated with decreased mortality in severe coronavirus disease 2019 patients with coagulopathy. J Thromb Haemost. 2020;18:1094-1099. [PMID: 32220112] doi:10.1111/jth.14817
32. **Bikdeli B, Madhavan MV, Jimenez D, et al.** COVID-19 and thrombotic or thromboembolic disease: implications for prevention, antithrombotic therapy, and follow-up. J Am Coll Cardiol. 2020. [PMID: 32311448] doi:10.1016/j.jacc.2020.04.031

AD LIBITUM

A Visit to Polk Institute

It was natural for us to visit the idiots
at Polk Institute. Though abuzz
with curiosity, we took it slowly.
First, morons playing table-top games
in the solarium bustled around us,
smiling. Next, came the imbeciles'
oversized faces in chairs at the foot
of their beds. Last, a cavernous hall
of cribs with idiots in them, babies
big enough to thicken our skins
with truth, an important precaution
for doctoring. Nothing is more natural,
the idiots told us, than imperfection,
and nothing is more solemn than silence.
We were aliens with tanks on our backs
containing a gas that protected us
from human feeling. We knew nothing.

Jack Coulehan, MD
Center for Medical Humanities, Compassionate Care, and Bioethics at Stony Brook University
Stony Brook, New York

Current Author Address: Jack Coulehan, MD;
e-mail, john.coulehan@stonybrookmedicine.edu.

Current Author Addresses: Drs. Wichmann, Burdelski, de Heer, Nierhaus, Frings, and Kluge: Department of Intensive Care Medicine, University Medical Center Hamburg-Eppendorf, Martinistr. 52, 20246 Hamburg, Germany.
Drs. Sperhake, Edler, Heinemann, Heinrich, Mushumba, Kniep, Schröder, and Püschel: Department of Legal Medicine, University Medical Center Hamburg-Eppendorf, Martinistr. 52, 20246 Hamburg, Germany.
Drs. Lütgehetmann, Pfefferle, and Aepfelbacher: Institute of Medical Microbiology Virology and Hygiene, University Medical Center Hamburg-Eppendorf, Martinistr. 52, 20246 Hamburg, Germany.
Dr. Steurer: Department of Pathology, University Medical Center Hamburg-Eppendorf, Martinistr. 52, 20246 Hamburg, Germany.
Dr. Becker: Department of Pulmonology and Internal Intensive Care, Asklepios Hospital Barmbek, Rübenkamp 220, 22307 Hamburg, Germany.
Dr. Bredereke-Wiedling: Emergency Department, Bethesda Hospital Bergedorf, Glindersweg 80, 21029 Hamburg, Germany.
Dr. de Weerth: Department of Internal Medicine, Agaplesion Diakonie Hospital, Hohe Weide 17, 20259 Hamburg, Germany.
Dr. Paschen: Department of Anesthesiology and Intensive Care, Amalie Sieveking Hospital, Haselkamp 33, 22359 Hamburg, Germany.
Dr. Sheikhzadeh-Eggers: Emergency Department, Asklepios Hospital Saint Georg, Lohmühlenstrasse 5, 20099 Hamburg, Germany.
Dr. Stang: Department of Oncology, Asklepios Hospital Barmbek, Rübenkamp 220, 22307 Hamburg, Germany.
Drs. Schmiedel and Addo: Sections of Infectious Diseases and Tropical Medicine, Department of Internal Medicine, University Medical Center Hamburg-Eppendorf, Martinistr. 52, 20246 Hamburg, Germany.
Dr. Bokemeyer: Department of Hematology and Oncology, Section of Pneumology, University Medical Center Hamburg-Eppendorf, Martinistr. 52, 20246 Hamburg, Germany.

Author Contributions: Conception and design: D. Wichmann, J.P. Sperhake, F. Heinrich, S. Kluge.
Analysis and interpretation of the data: D. Wichmann, J.P. Sperhake, M. Lütgehetmann, S. Steurer, F. Heinrich, H. Mushumba, I. Kniep, A.S. Schröder, A. de Weerth, C. Bokemeyer, M.M. Addo, M. Aepfelbacher, S. Kluge.
Drafting of the article: D. Wichmann, J.P. Sperhake, M. Lütgehetmann, I. Kniep, S. Kluge.
Critical revision for important intellectual content: D. Wichmann, J.P. Sperhake, I. Kniep, C. Burdelski, G. de Heer, A. Nierhaus, A. de Weerth, A. Stang, S. Schmiedel, M.M. Addo, M. Aepfelbacher, S. Kluge.
Final approval of the article: D. Wichmann, J.P. Sperhake, M. Lütgehetmann, S. Steurer, C. Edler, A. Heinemann, F. Heinrich, H. Mushumba, I. Kniep, A.S. Schröder, C. Burdelski, G. de Heer, A. Nierhaus, D. Frings, S. Pfefferle, H. Becker, H. Bredereke-Wiedling, A. de Weerth, H. Paschen, S. Sheikhzadeh-Eggers, A. Stang, S. Schmiedel, C. Bokemeyer, M.M. Addo, M. Aepfelbacher, K. Püschel, S. Kluge.
Provision of study materials or patients: D. Wichmann, A. Heinemann, F. Heinrich, H. Mushumba, C. Burdelski, G. de Heer, A. de Weerth, S. Sheikhzadeh-Eggers, C. Bokemeyer, M.M. Addo, K. Püschel.
Statistical expertise: S. Kluge.
Obtaining of funding: M. Aepfelbacher.
Administrative, technical, or logistic support: D. Wichmann, J.P. Sperhake, S. Steurer, C. Edler, A. Heinemann, F. Heinrich, A.S. Schröder, C. Burdelski, M.M. Addo, S. Kluge.
Collection and assembly of data: D. Wichmann, J.P. Sperhake, M. Lütgehetmann, S. Steurer, C. Edler, F. Heinrich, H. Mushumba, I. Kniep, A.S. Schröder, G. de Heer, A. Nierhaus, D. Frings, S. Pfefferle, H. Becker, H. Bredereke-Wiedling, A. de Weerth, H.R. Paschen, A. Stang, S. Schmiedel, K. Püschel, S. Kluge.

Appendix Figure 1. Thrombosis of the prostatic vein (case 1) (*arrows*).

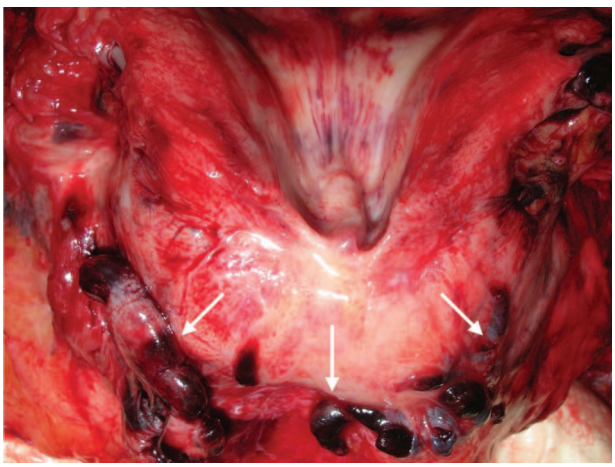

Appendix Table 1. Weights of Individual Organs, in Grams, for All Cases*

Case Number	Brain	Heart	Lung (Right)	Lung (Left)	Liver	Kidney (Right)	Kidney (Left)	Spleen
1	1520	660	1135	940	3880	215	305	500
2	1430	515	1220	1030	2030	155	155	355
3	1665	510	1280	1445	1930	240	240	280
4	1435	605	1370	1100	2180	210	210	240
5	1450	360	955	845	1645	180	165	310
6	950	250	275	275	890	80	90	90
7	1210	415	690	655	1380	105	120	95
8	1170	575	1160	940	1610	145	160	260
9	1080	355	480	410	715	100	35	50
10	1350	390	730	630	945	115	145	135
11	1400	650	1880	1540	1450	225	240	240
12	1460	745	1580	1290	2265	270	220	360

* Weights are rounded to 5 g. Standard weights for men and women (adopted from Molina and DiMaio [13, 14]), respectively, are as follows (the dependence of standard organ weights on body weight was not considered here): brain, 1401 g and 1233 g; heart, 331 g and 245 g; lung (right), 445 g and 340 g; lung (left), 395 g and 299 g; liver, 1561 g and 1288 g; kidney (right), 129 g and 108 g; kidney (left), 137 g and 116 g; and spleen, 139 g and 115 g.

Appendix Table 2. Macroscopic Autopsy Findings in Organs Other Than the Lung in Patients Dying of COVID-19*

Case Number	Heart	Liver	Kidneys	Spleen	Prostate	Veins	Bowel	Pharynx	Adrenal Glands	Arteries	Miscellaneous
1	Excentric hypertrophy of both ventricles	Hepatomegaly	Shock kidneys	Splenomegaly	Thrombosis	Thrombosis	Ischemic enterocolitis	Normal	Normal	Atherosclerosis	–
2	CHD with stenting, status post MI, cardiac aneurysm, hypertrophy	Shock liver	Normal	Enlarged	Status post prostatectomy	Normal	Normal	Normal	Normal	Atherosclerosis	–
3	Biventricular hypertrophy, moderate CHD	Shock liver	Normal	Normal	Thrombosis, benign hypertrophy	Thrombosis, phlebosclerosis	Diverticulosis, ischemic enterocolitis	Normal	Micronodular hyperplasia	Atherosclerosis	Status post VATS (resection of right upper lung lobe)
4	Left ventricular hypertrophy	Shock liver	Normal	Normal	Thrombosis	Thrombosis	Ischemic colitis	Normal	Normal	Slight atherosclerosis	Struma colloides nodosa
5	CHD, status post MI	Normal	Normal	Normal	Thrombosis	Thrombosis	Status post abdominal surgery	Normal	Normal	Slight atherosclerosis	–
6	Normal	Normal	Old infarctions/chronic inflammation, nephrolithiasis	Normal	–	Normal	Adenoma of the duodenum	Normal	Adenoma	Normal	Trisomy 21, PEG tube, cholezystolithiasis, small brain, umbilical hernia
7	CHD, moderate hypertrophy, calcification of the mitral ring, status post MI, pacemaker, lipomatosis cordis	Normal	Normal	Normal	–	Normal	Normal	Normal	Micronodular hyperplasia	Atherosclerosis	Anasarca, cholezystolithiasis
8	CHD, status post bypass surgery, status post MI, cardiac aneurysm, global hypertrophy	Chronic congestion	Cysts	Chronic congestion	Thrombosis, benign hypertrophy	Thrombosis	Diverticulosis of the small bowel	Normal	Normal	Atherosclerosis	Cerebral sclerosis, status post cholecystectomy
9	Left atrial dilatation, CHD, status post MI	Fatty change	Shrinkage (left kidney)	Nonspecific acute splenitis	–	Normal	Pseudomembranous colitis	Normal	Normal	Atherosclerosis	NET of the lungs, osteoporosis
10	CHD, status post MI	Normal	Arteriosclerosis, atrophy, cysts	Nonspecific acute splenitis	Benign hypertrophy	Normal	Normal	Normal	Normal	Slight atherosclerosis	Suspected septic encephalomalacia (brain dissection pending), pancreatic fibrosis, cholezystolithiasis
11	CHD, status post aortic valve replacement, biventricular hypertrophy	Normal	Normal	Normal	Status post prostatectomy	Thrombosis	Normal	Normal	Micronodular hyperplasia	Atherosclerosis	–
12	CHD, hypertrophy	Chronic congestion, fatty changes	Multiple cysts	Chronic congestion	Benign hypertrophy, thrombosis	Thrombosis	Normal	Normal	Micronodular hyperplasia	Atherosclerosis	Cerebral sclerosis, hemorrhagic cystitis

CHD = coronary heart disease; MI = myocardial infarction; NET = neuroendocrine tumor; PEG = percutaneous endoscopic gastrostomy; VATS = video-assisted thoracoscopic surgery.
* No abnormal findings were present in the testes or ovaries of any patient.

Appendix Figure 2. Mononuclear infiltrations consisting of lymphocytes (*arrows*) in the myocardium of the right ventricle (case 3) (hematoxylin–eosin stain; original magnification, × 100).